Accurate Calibration of a Fringe Projection System by Considering Telecentricity

Dipl.-Ing. Klaus Haskamp [a, d], Dr.-Ing. Dipl.-Phys Markus Kästner [b, d], Prof. Dr.-Ing Eduard Reithmeier[c, d]

[a]Research Associate in the workgroup Production Metrology;
[b]Head of the workgroup Production Metrology;
[c]Head of the Institute of Measurement and Automatic Control;
[d]Institute of Measurement and Automatic Control, Leibniz Universität Hannover, Nienburger Strasse 17, Hannover, Germany

ABSTRACT

Fringe projection systems can be used for the measurement of complex workpiece geometries. Virtual fringe projection systems can be used for the calculation of optimal measurement strategies with respect to criteria like a minimal measurement uncertainty. This is the main field of research of the subproject B5 of the collaborative research centre 489 (CRC 489), funded by the German Research Foundation (DFG). The main task of the subproject is to develop a virtual multisensor assistance system for the calculation of workpiece adapted measurement strategies. This paper focuses on the model and calibration of the used fringe projection sensor.

The sensor has to be modelled and the system parameters have to be identified by an accurate calibration procedure. The used fringe projection system has a camera lens with an object-sided telecentricity. Usually, the components projector and camera were described using a pinhole model, which does not reflect the telecentricity. This means, that the existing physical formulations and calibration procedures cannot be used, here.

In this paper, the model and calibration strategy for the calculation of the system parameters are described in detail. In order to get a precise simulation model, each intrinsic and extrinsic parameter is considered. To verify the virtual model and the calibration strategy, the calibration was repeated and the standard deviation of the parameters was calculated. Furthermore an optical flat and a groove artefact will be measured and the planarity of the optical flat and the depth of the groove artefact will be determined and compared to the calibrated values.

Keywords: Virtual Multisensor Assistance System, Virtual Fringe Projection, Physical Model, Calibration Strategy, Object-sided Telecentricity

1. INTRODUCTION

Fringe projection systems are qualified for the measurement of complex workpiece geometries due to the short measurement times and the high point density. For an accurate measurement it is necessary to calibrate the sensor. This can be done by the use of black box methods or with a model based approach. Examples for black box methods are a polynomial formulation or neural networks. The model based approach is based on physical backgrounds and tries to describe the real sensor behaviour by regarding the intrinsic and extrinsic parameters.

The main advantage of the use of black box methods is, that there has to be no knowledge about the real sensor behaviour. Usually, this method is applied for systems, whose structure is to complex in order to be described with physics. A major disadvantage is, that there is no information, how much the single system parameters (polynomial coefficients, activation function, weighting coefficients) have an effect on the measurement accuracy.

The main advantage of the model based approach is, that there is a completely virtual model with the physical sensor properties. The physical model of the sensor can be used for statistical analysis. For example, the influence of the system parameters concerning the measurement uncertainty can be estimated. Another

Further author information: (Send correspondence to Klaus Haskamp)
Klaus Haskamp: E-mail: klaus.haskamp@imr.uni-hannover.de, Telephone: +49 (0)511 762 42 84

Optical Measurement Systems for Industrial Inspection VII, edited by Peter H. Lehmann, Wolfgang Osten, Kay Gastinger, Proc. of SPIE Vol. 8082, 80821B · © 2011 SPIE
CCC code: 0277-786X/11/$18 · doi: 10.1117/12.888037

field of application is the use of the virtual model as part of a virtual multisensor assistance system for the calculation of intelligent and workpiece specific measurement strategies with respect to different criteria, like minimal measurement time or measurement uncertainty. This is the main field of research of the subproject B5 "Complete Geometry Inspection" of the collaborative research centre 489 (CRC 489) "Process Chain for the Production of Precision Forged High Performance Components", funded by the German Research Foundation (DFG).

The main task of the subproject is to develop a virtual multisensor assistance system, build up from a shadow projection sensor, composed of with a linear and a rotational axis, and a fringe projection sensor, which is fixed on a 3 DOF (Degree of Freedom) positioning system. The virtual system is applied for the estimation of measurement uncertainties for a certain workpiece alignment in the measurement volume. Based on the uncertainty estimation, it is intended to calculate the best workpiece orientation and position, so that an optimal measurement is accomplished for the geometric tolerances. Thereby, the optimisation criteria are a minimal measurement time, a measurement with a minimal uncertainty and a holistic measurement. Besides the integration of the named criteria, the measurement device of the existing assistance system, which is the most suitable device for the measurement task, should be determined.

The focus of this paper lies on the description of the physical and mathematical model of a fringe projection sensor and the model adapted calibration procedure. It is necessary to describe each relevant physical effect in the model and to identify all system parameters with a very high accuracy, if the virtual measurement system should be used for statistical analysis. The camera lens of the used fringe projection system has an object-sided telecentricity. Usually, this is not considered in the physical model and calibration strategies. To get a more precise virtual model, this influence has to be taken into account. This means, that existing physical formulations of fringe projection systems and developed calibration strategies cannot be used for this case.

In this paper the virtual model and the calibration procedure for the estimation of all system parameters should be explained in detail. In Sec. 2 the physical model of the fringe projection system is presented. Thereby all intrinsic and extrinsic parameters will be considered. Examples for intrinsic parameters are distortion parameters and the displacement of the image focal point. The relative position and orientation of the optical axis of the camera lens and the projector lens with respect to the inertial world coordinate system (object coordinate system) or the object-sided telecentricity of the camera lens are extrinsic parameters. After the formulation of the virtual system, the calibration procedure for the identification of all system parameters will be described and discussed in Sec. 3.1 and in Sec. 3.2. In Sec. 4 the verification of the used model and the calibration strategy will be given. An optical flat and a groove artefact will be measured in different positions and the planarity of the optical flat and the depth of the groove artefact will be determined and compared to the calibrated values, which is written in Sec. 4.1 and in Sec. 4.2.

2. VIRTUAL MODEL OF THE FRINGE PROJECTION SYSTEM

In this chapter, the virtual model of the fringe projection system should be explained. The virtual model is based on the fundamentals of projective geometry, which allows a compact description of transformations.[1,2] Usually, the projective geometry is used for the description of cameras. Due to the fact, that a projector can be treated as an inverse camera, the projective geometry can be used for the description of the projector.[3] The used fringe projection system is build from one camera, which has an object-sided telecentricity, and one projector. The transformation steps between the image coordinate system and the object coordinate system is described for the camera in Sec. 2.1 and for the projector in Sec. 2.2.

2.1 Virtual model of the camera

The homogenous transformation of a homogenous 3D-point $\mathbf{X} = [x, y, z, 1]$ onto a homogen 2D-point $\eta = [i, j, 1]$ is done in homogenous coordinates. It is useful to define a global coordinate system for the following considerations. This coordinate system is called the object coordinate system CS_{Obj} and is positionend in the middle of the measurement volume.[4] The affiliation of the points belonging to the respective coordinate system is expressed with the postpositonend short form of the name of the CS, e.g. $\mathbf{X}_{Obj}$.

The virtual model of the used fringe projection system is shown in Fig. 1. Following, the transformation from the object coordinate system CS_{Obj} into the coordinate system of the CCD CS_{CCD}, the pixel coordinate system,

will be described. In the first step, $\mathbf{X}_{Obj}$ is projected into the so called component coordinate system CS_{Comp}, which is positionend in the middle of the camera lens. Thereby $\mathbf{T}_{Obj}^{Comp}$ is the so called extrinsic matrix:[2]

$$\mathbf{T}_{Obj}^{Comp} = \begin{bmatrix} \mathbf{R}_{Obj}^{Comp} & \mathbf{r}_{Obj} \\ \mathbf{0}^T & 1 \end{bmatrix} \quad \text{with} \quad \mathbf{X}_{Comp} = \mathbf{T}_{Obj}^{Comp} \cdot \mathbf{X}_{Obj} \ , \tag{1}$$

with $\mathbf{R}_{Ob}^{Comp}$ as the rotation part, $\mathbf{r}_{Obj}$ as the translatorial part of $\mathbf{T}_{Obj}^{Comp}$ and $\mathbf{0}^T$ as a transposed zero vector. For the transformation from CS_{Comp} into CS_{Obj} the following formula can be used:

$$\mathbf{T}_{Comp}^{Obj} = \begin{bmatrix} \left(\mathbf{R}_{Obj}^{Comp}\right)^T & -\left(\mathbf{R}_{Obj}^{Comp}\right)^T \cdot \mathbf{r}_{Obj} \\ \mathbf{0}^T & 1 \end{bmatrix} \quad \text{with} \quad \mathbf{X}_{Obj} = \mathbf{T}_{Comp}^{Obj} \cdot \mathbf{X}_{Comp} \ . \tag{2}$$

In our case we assume, that the orientation between CS_{Obj} and CS_{Comp} is equal and that there is only a translatorial element in the z-direction:

$$\mathbf{T}_{Obj}^{Comp} = \begin{bmatrix} 1 & 0 & 0 & 0 \\ 0 & 1 & 0 & 0 \\ 0 & 0 & 1 & z_{Cam} \\ 0 & 0 & 0 & 1 \end{bmatrix} . \tag{3}$$

The parameter z_{Cam} is neglected during the calibration procedure due to the fact, that the projection is telecentric.

In the next step $\mathbf{X}_{Comp}$ is transformed into the image coordinate system CS_{Image} using a telecentric projection matrix:[1]

$$\mathbf{K}_Z = \begin{bmatrix} 1 & 0 & 0 & 0 \\ 0 & 1 & 0 & 0 \\ 0 & 0 & 0 & 1 \end{bmatrix} \quad \text{with} \quad \mathbf{X}_{Image} = \mathbf{K}_Z \cdot \mathbf{X}_{Comp} \ . \tag{4}$$

$\mathbf{K}_Z$ describes a projection from a 3D-space into a 2D-space with the rank 3. This means, that there exists no direct transformation from $\mathbf{X}_{Image}$ into $\mathbf{X}_{Comp}$.[4] The matrix $\mathbf{T}_{Image}^{Comp}$ is calculated with the pseudo inverse according to "Moore-Penrose":[5]

$$\mathbf{K}_{Z,inv} = \mathbf{K}_Z^T \cdot \left(\mathbf{K}_z \cdot \mathbf{K}_Z^T\right)^{-1} = \begin{bmatrix} 1 & 0 & 0 \\ 0 & 1 & 0 \\ 0 & 0 & 0 \\ 0 & 0 & 1 \end{bmatrix} \quad \text{with} \quad \mathbf{X}_{Comp} = \mathbf{K}_{Z,inv} \cdot \mathbf{X}_{Image} \ . \tag{5}$$

The optical components are not optimal and have aberrations. Usually, the aberrations were seperated into the following distortion groups:[6,7]

$$\text{radial symmetric: } \delta\mathbf{x}_r = \begin{bmatrix} \delta x_r & \delta y_r \end{bmatrix} = \mathbf{f}_r\left(k_1, k_2, k_3\right), \tag{6}$$

$$\text{radial asymmetric: } \delta\mathbf{x}_d = \begin{bmatrix} \delta x_d & \delta y_d \end{bmatrix} = \mathbf{f}_d\left(p_1, p_2\right), \tag{7}$$

$$\text{affinity and shear: } \delta\mathbf{x}_a = \begin{bmatrix} \delta x_a & \delta y_a \end{bmatrix} = \mathbf{f}_a\left(A_1, A_2\right). \tag{8}$$

k_1, k_2, k_3, p_1, p_2, A_1 and A_2 are the distortion parameters and were summarized in the vector $\mathbf{k}$ and r is the radius.

The distortion function $\mathbf{L}$ summarizes the distortions and is used for the projection from the image coordinate system CS_{Image} into the distorted image coordinate system $CS_{Image'}$:

$$\mathbf{X}_{Image'} = \mathbf{L}\left(\mathbf{X}_{Image}, \mathbf{k}\right). \tag{9}$$

For the transformation from $CS_{Image'}$ to CS_{Image}, the inverse distortion function $\mathbf{L}^{-1}$ has to be calculated:

$$\mathbf{X}_{Image} = \mathbf{L}^{-1}\left(\mathbf{X}_{Image'}, \mathbf{k}\right). \tag{10}$$

Due to the fact, that $\mathbf{L}$ is a nonlinear function, there exist no direct conversion of $\mathbf{L}^{-1}$ and nonlinear optimisation algorithms, such as the "Nelder-Mead-" or the "Rosenbrock-procedure", have to be used to calculate $\mathbf{X}_{Image}$.

In the next step the points were transformed onto the sensor coordinate system CS_{Sensor}:

$$\mathbf{T}_{Image'}^{Sensor} = \begin{bmatrix} c & 0 & 0 \\ 0 & c & 0 \\ 0 & 0 & 1 \end{bmatrix} \quad \text{with} \quad \mathbf{X}_{Sensor} = \mathbf{T}_{Image'}^{Sensor} \cdot \mathbf{X}_{Image'} \ , \tag{11}$$

with c as a constant. The inverse of $\mathbf{T}_{Image'}^{Sensor}$ can be used for the inverse transformation:

$$\mathbf{T}_{Sensor}^{Image'} = \begin{bmatrix} \frac{1}{c} & 0 & 0 \\ 0 & \frac{1}{c} & 0 \\ 0 & 0 & 1 \end{bmatrix} \quad \text{with} \quad \mathbf{X}_{Image'} = \mathbf{T}_{Sensor}^{Image'} \cdot \mathbf{X}_{Sensor} \ . \tag{12}$$

In the last step the points were projected into the coordinate system of the CCD CS_{CCD}:

$$\mathbf{T}_{Sensor}^{CCD} = \begin{bmatrix} 1 & 0 & \frac{b_{CCD}}{2} \\ 0 & 1 & \frac{h_{CCD}}{2} \\ 0 & 0 & 1 \end{bmatrix} \quad \text{with} \quad \mathbf{X}_{CCD} = \mathbf{T}_{Sensor}^{CCD} \cdot \mathbf{X}_{Sensor} \ , \tag{13}$$

with b_{CCD} as the width and h_{CCD} as the height of the CCD-matrix. After that, the points $\mathbf{X}_{CCD}$ were converted into discrete pixels. The transformation from CS_{CCD} into CS_{Sensor} can be done with the following formula:

$$\mathbf{T}_{CCD}^{Sensor} = \begin{bmatrix} 1 & 0 & -\frac{b_{CCD}}{2} \\ 0 & 1 & -\frac{h_{CCD}}{2} \\ 0 & 0 & 1 \end{bmatrix} \quad \text{with} \quad \mathbf{X}_{Sensor} = \mathbf{T}_{CCD}^{Sensor} \cdot \mathbf{X}_{CCD} \ . \tag{14}$$

Altogether, there are the following unknown parameters, which have to be identified during the calibration procedure:

- intrinsic parameters: $k_1, k_2, k_3, p_1, p_2, A_1, A_2$,
- extrinsic parameters: c.

2.2 Virtual model of the projector

The whole transformation for the projection from CS_{Obj} into the coordinate system of the DMD CS_{DMD} is very similar to Sec. 2.1. In this chapter, only the differences should be explained.

In the first step, the translatorial and the rotational part of $\mathbf{T}_{Comp}^{Obj}$ is considered:

$$\mathbf{T}_{Obj}^{Comp} = \begin{bmatrix} \mathbf{R}_{Obj}^{Comp} & \mathbf{r}_{Obj} \\ \mathbf{0}^T & 1 \end{bmatrix} \quad \text{with} \quad \mathbf{X}_{Comp} = \mathbf{T}_{Obj}^{Comp} \cdot \mathbf{X}_{Obj}, \tag{15}$$

$$\mathbf{R}_{Obj}^{Comp} = \mathbf{R}_z\left(\phi\right) \cdot \mathbf{R}_y\left(\psi\right) \cdot \mathbf{R}_x\left(\theta\right) \quad \text{and} \quad \mathbf{r}_{Obj} = \begin{bmatrix} x_{proj} & y_{Proj} & z_{proj} \end{bmatrix} \ , \tag{16}$$

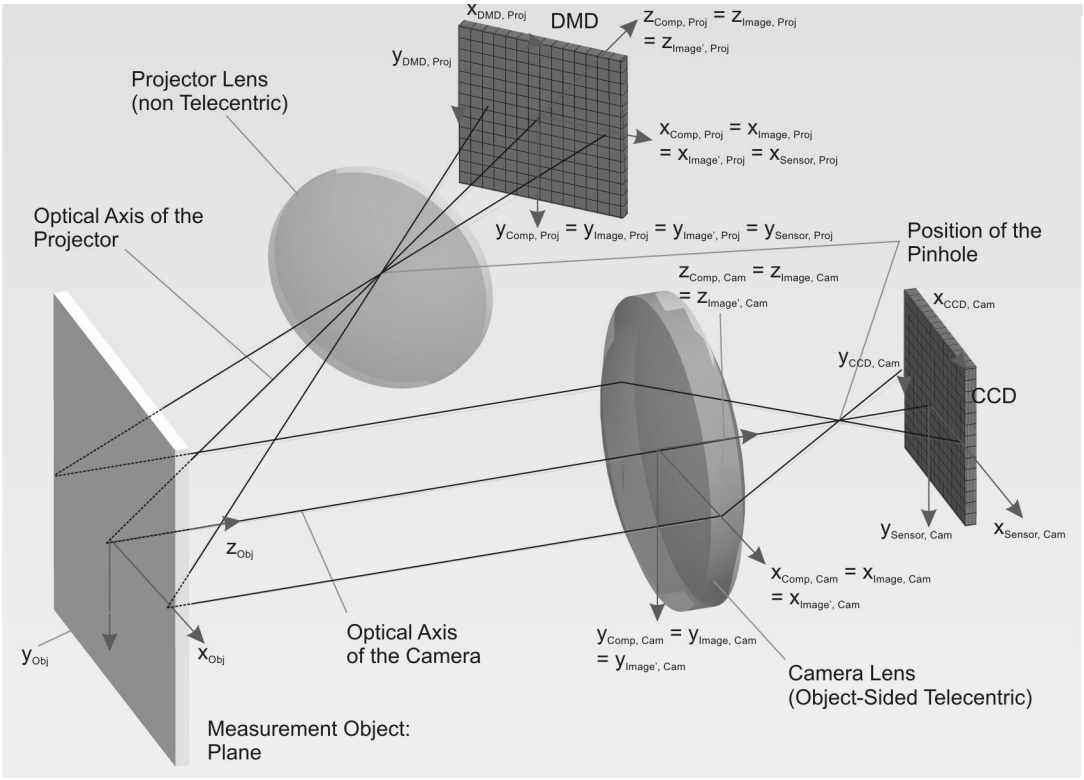

Figure 1. Principle of the used fringe projection system

with $\mathbf{R}_z(\phi)$ as the rotation matrix concerning the z-axis, $\mathbf{R}_y(\psi)$ as the rotation matrix concerning the y-axis and $\mathbf{R}_x(\theta)$ as the rotation matrix concerning the x-axis. This means, that there are 6 more unknown parameters $(\theta, \psi, \phi, x_{Proj}, y_{Proj}, z_{Proj})$ compared to the camera model.

The next difference is, that there exists no transformation between the distorted image coordinate system $CS_{Image'}$ and the sensor coordinate system CS_{Sensor}. Therewith $\mathbf{T}_{Image'}^{Sensor}$ and $\mathbf{T}_{Sensor}^{Image'}$ are neglected.

The third variation in the transformation is the consideration of the displacement of the image focal point:

$$\mathbf{T}_{Sensor}^{DMD} = \begin{bmatrix} 1 & 0 & \frac{b_{DMD}}{2} - x_0 \\ 0 & 1 & \frac{h_{DMD}}{2} - y_0 \\ 0 & 0 & 1 \end{bmatrix} \quad \text{with} \quad \mathbf{X}_{DMD} = \mathbf{T}_{Sensor}^{DMD} \cdot \mathbf{X}_{Sensor} \ , \tag{17}$$

with x_0 and y_0 as the position of the image focal point.

Furthermore the position of the pinhole $\mathbf{X}_{Pin} = \begin{bmatrix} x_{Pin} & y_{Pin} & z_{Pin} \end{bmatrix}$ must be considered. The position is necessary for the construction of the rays, which start from the DMD in the direction of the measurement object. This will be explained in Sec. 3.2.

In total, there are the following unknown system parameters:

- intrinsic parameters: $k_1, k_2, k_3, p_1, p_2, A_1, A_2, x_0, y_0$,
- extrinsic parameters: $\theta, \psi, \phi, x_{Proj}, y_{Proj}, z_{Proj}, x_{Pin}, y_{Pin}, z_{Pin}$.

3. CALIBRATION PROCEDURE

In this chapter the calibration procedure for the identification of all system parameters is explained in detail. Due to the fact, that a calibrated camera is necessary for the calibration of the projector, at first the method for the identification of the camera parameters is presented in Sec. 3.1. Sec. 3.2 deals with the method of the projector calibration.

3.1 Calibration procedure for the estimation of the camera parameter

The camera calibration is done with a chessboard with an edge size of $1mm$, as shown in Fig. 2. Additionally, four squares are positionend in the edges of the chessboard and used for the automatic edge point detection. Due to the fact, that the projector is calibrated with the same pattern, the color of the sqaures are magenta and yellow. Therefore, it is possible to seperate the pattern, which was send out from the projector, from the pattern, shown in Fig. 2, in the camera image.

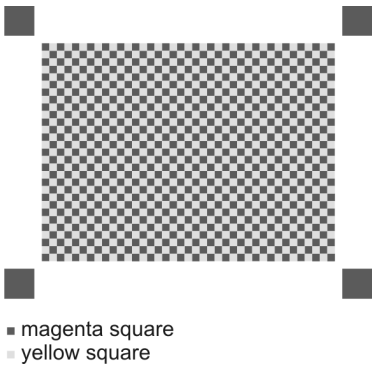

Figure 2. Used calibration chessboard

Previous to the rather calibration, the edge points were detected in the camera image and a periodical pattern, the reference pattern, was created. The edge points, found in the camera image, are called the imaged points p_{imaged} and the points from the periodical pattern are named the reference points p_{ref}. The equidistant distance between the points from p_{ref} is $1mm$. For the reason, that the projection is telecentric, the information of the position and orientation of the calibration chessboard with respect to the object coordinate system is lost. Furthermore, the imaged pattern is displaced with respect to the x- and y- axis of CS_{Obj}. This means, that 5 more parameters, the rotation angles θ, ψ, ϕ among the x-, y- and z-axis and the displacement, Δx and Δy, concerning the x- and the y-axis of the object coordinate system, have to be identified. Following these parameters were called the external parameters and summarized in the vector $\mathbf{x}_{ex}$.

The principle of the calibration is shown in Fig. 3. The reference pattern is rotated and tilted using θ, ψ and ϕ. In the following, the new oriented pattern is displaced with Δx and Δy. In the next step, the lens distortion is calculated for each point, using $\mathbf{k}$ and $\mathbf{L}$. In the last step, the distorted points were transformed onto the CCD-coordinate system CS_{CCD} and converted into discrete pixels, so that $p_{ref,trans}$ is available for futher analysis. For the definition of the calibration functional ϵ, the projected points $p_{ref,trans}$ were compared with the points p_{imaged}:

$$\epsilon = \|p_{ref,trans} - p_{imaged}\|^2 = f(\mathbf{p}) \quad \wedge \quad \min_{\mathbf{p}}(f) \Rightarrow \mathbf{p} \ , \tag{18}$$

with $\mathbf{p}$ as the parameter vector. The minimum of the function f can be found using nonlinear optimisation algorithms, because of the nonlinear character of f.

The aim of the calibration procedure is to find the parameters $\mathbf{k}$ and c and, additionally for each image, $\mathbf{x}_{ex}$, which transform the reference onto the measured pattern and minimise the deviation ϵ. The calibration procedure is designed as a multi-step calibration. This means, that the parameters in Equation (18) differ in

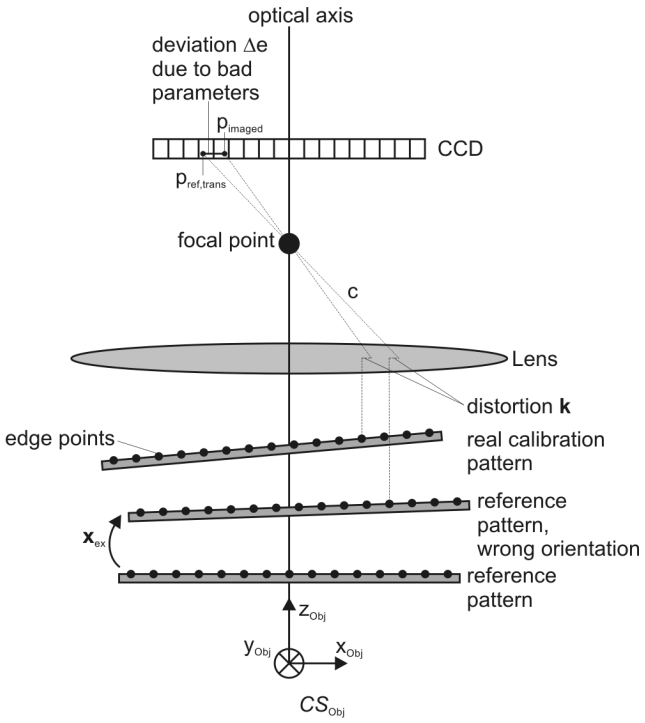

Figure 3. Calibration principle

the single steps. In the first step, $\mathbf{p}$ is equal with $\mathbf{x}_{ex}$ and $\mathbf{k}$ and c are constant values. In the second step, the distortion parameters $\mathbf{k}$ are the variables and $\mathbf{x}_{ex}$, which was calculated before, and c are constant. In the last step, the transformation parameter c is the unknown parameter, whereas $\mathbf{k}$ and $\mathbf{x}_{ex}$ are constant. The three steps were executed until a maximum number of iteration steps is reached or the function value of ϵ decreases under a pre-defined barrier. For the start of the multi-step-calibration, the parameters $\mathbf{k}$, c and $\mathbf{x}_{ex}$ were set to start values. Thereby it is assumed, that the lens is a perfect lens without distortion and that the calibration pattern is parallel to the x- and y-plane of CS_{Obj} without a displacement:

$$\mathbf{k} = \mathbf{0} \quad \wedge \quad \mathbf{x}_{ex} = \mathbf{0} \ . \tag{19}$$

c_{start} was set to 1.

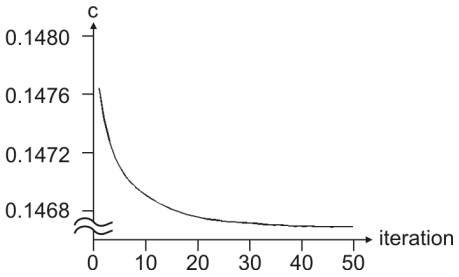

Figure 4. Behaviour of the parameter c during the iteration steps

In Fig. 4 the behaviour of the value of the parameter c during the iteration steps is shown. It can be seen, that the value is stable for a number of 40 iterations. This result could be found for the other parameters, too. The calibration procedure has been repeated 20 times. The mean value and the standard deviation of the identified parameters are shown in the Tab. 1.

Table 1. Mean value and standard deviation of the identified parameters

	$c[/]$	$k_1[/]$	$k_2[/]$	$k_3[/]$
Mean value	0.14676641	$-5.469625 \cdot 10^{-6}$	$3.004999 \cdot 10^{-8}$	$-3.333333 \cdot 10^{-11}$
Standard deviation	0.00002682	$6.779677 \cdot 10^{-8}$	$2.705628 \cdot 10^{-8}$	$4.923659 \cdot 10^{-11}$
	$p_1[/]$	$p_2[/]$	$A_1[/]$	$A_2[/]$
Mean value	$-5.469625 \cdot 10^{-6}$	$3.004999 \cdot 10^{-8}$	0.006422	$9.564834 \cdot 10^{-4}$
Standard deviation	$6.779677 \cdot 10^{-6}$	$2.705628 \cdot 10^{-8}$	$1.033259 \cdot 10^{-6}$	$2.983822 \cdot 10^{-4}$

The table points out, that the standard deviation of the parameters k_2, k_3, p_1 and p_2 has the same magnitude as the mean value. This implies, that the parameters should not be regarded in the virtual model. In Fig. 5 the histogramm of the calibration error in Pixel and the error map in Pixel is shown. The figure points out, that most of the calibration errors are less than 1 pixel. This means, that the calibration was successful.

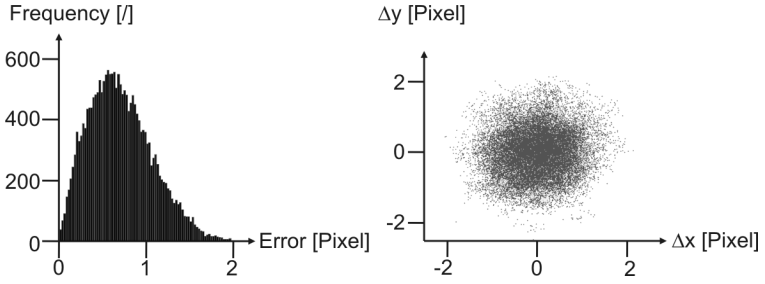

Figure 5. Histogramm and error map from the calibration error after the calibration

3.2 Calibration procedure for the estimation of the projector parameter

Three different images were used for the calibration of the projector. The first pattern is the pattern from the camera calibration, shown in Fig. 2. This pattern is necessary for the calculation of the orientation of the plane with respect to the object coordinate system. The other two images were shown in Fig. 6 and were projected from the projector onto the reference plane. Due to the fact, that the colors of the squares of the calibration chessboard are magenta and yellow, it is possible, to detect the edge points of the patterns, projected from the projector. The calibration chessboard is placed in different positions in the object coordinate systems. In each position, the three patterns were imaged from the camera. For the identification, it is necessary, that the calibration chessboards are parallel and that the distances between the positions are known. In this case, this was realized using a x-y-positioning stage with a resolution of $10\mu m$ in the x-direction and of $10\mu m$ in the y-direction.

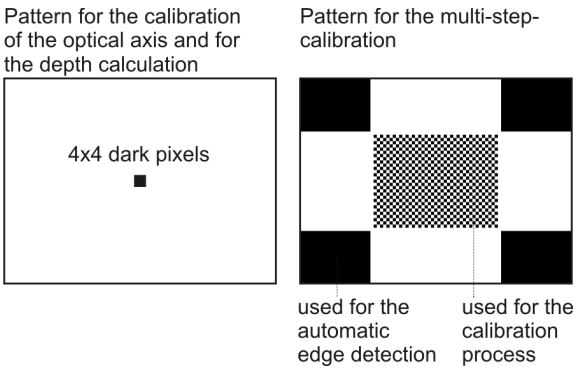

Figure 6. Used calibration patterns for the projector calibration

The calibration procedure is seperated into two different parts. In the first part, the orientation of the optical axis and therewith the parameters θ, ψ and ϕ, were calculated using the image, shown in the left side from Fig. 6. The projected pattern has $4x4$-dark pixels in the middle, which locates the optical axis of the projector in the camera image. Furthermore, the depth information from the position of the calibration chessboard with respect to the object coordinate system (z-position) is estimated. The second part is constructed as a multi-step-calibration, like the camera calibration procedure.

Previous to the start of the projector calibration, the edges from the calibration chessboard and the projected patterns from the projector (onto the calibration chessboard) were detected in the CCD-coordinate system of the camera. In the following, all edge points were transformed into the object coordinate system using the identified camera parameters. Because of the telecentricity of the camera lens, the depth information is missing. The estimation of the depth is explained later. The transformed edge points of the calibration chessboard are used to calculate the orientation (θ, ψ, ϕ) concerning the object coordinate system. In the following, the transformed edge points from the pattern, projected from the projector, were rotated and tilted using (θ, ψ, ϕ).

The principle for the calculation of the optical axis and the depth is shown in Fig. 7. A straight line is constructed for each position of the chessboard. The receiving point of the straight line is the transformed edge point of the pattern, shown in Fig. 6. The direction vector is the optical axis. The intersection points from the straight lines and the y-z-plane of the object coordinate system is the shift of the plane of the chessboard. In one case, the calculated optical axis is not equal to the real optical axis. For this reason, the shift is calculated erroneous and the distances between the shifted planes are not equal to the known distances. In the other case, the calculated optical axis is equal to the real optical axis. This means, that the correct shift is calculated and that the distances between the shifted planes of the chessboard are equal to the known distances. The parameter, which indicates a wrong or correct optical axis, is thereby the error between the calculated and the known distances. After the identifiaction of the optical axis, the depth information Δz is available for the multi-step-calibration.

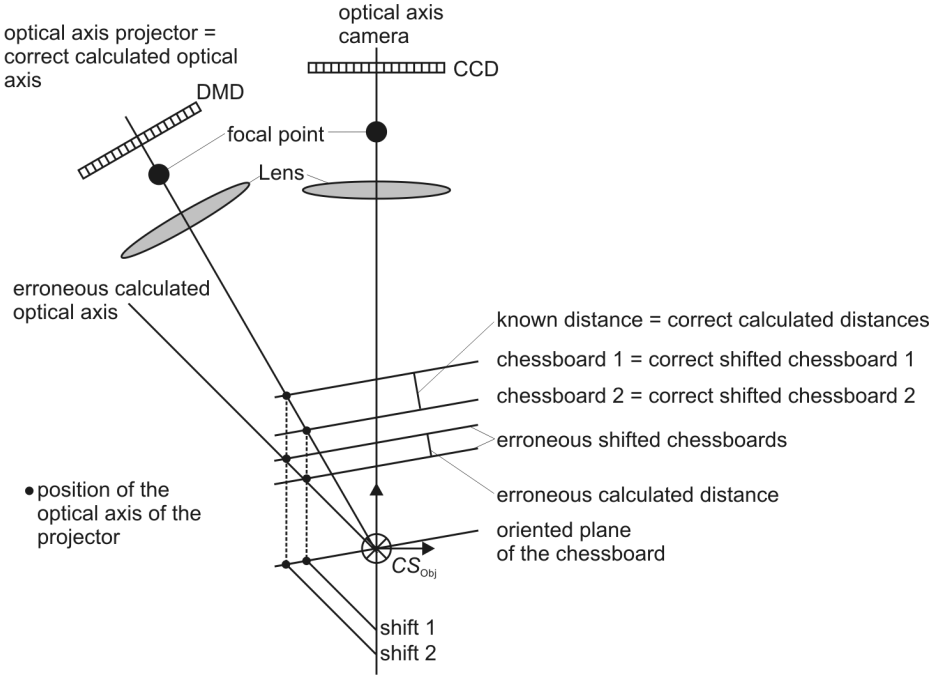

Figure 7. Principle for the calculation of the optical axis and the depth

For the start of the multi-step-calibration, the transformed edge points of the pattern, shown in the right side if Fig. 6, are shifted using the calculated shifts Δz. Furthermore, the parameters have to be initialised. It

Table 2. Mean value and standard deviation of the identified parameters

	$k_1[/]$	$k_2[/]$	$k_3[/]$	$p_1[/]$
Mean value	$-9.204991 \cdot 10^{-4}$	$3.322022 \cdot 10^{-8}$	$2.450282 \cdot 10^{-7}$	$-7.852697 \cdot 10^{-9}$
Standard deviation	$1.388103 \cdot 10^{-4}$	$4.345412 \cdot 10^{-8}$	$1.985247 \cdot 10^{-7}$	$6.652185 \cdot 10^{-9}$
	$p_2[/]$	$A_1[/]$	$A_2[/]$	$x_0[mm]$
Mean value	$4.342621 \cdot 10^{-8}$	$6.376495 \cdot 10^{-2}$	$2.393739 \cdot 10^{-2}$	$4.266255 \cdot 10^{-2}$
Standard deviation	$5.875965 \cdot 10^{-8}$	$2.781488 \cdot 10^{-3}$	$1.089107 \cdot 10^{-3}$	$6.621792 \cdot 10^{-4}$
	$y_0[mm]$	$x_{Pin}[mm]$	$y_{Pin}[mm]$	$z_{Pin}[mm]$
Mean value	$7.740350 \cdot 10^{-1}$	187.233499	-1.765159	217.144906
Standard deviation	$5.839153 \cdot 10^{-4}$	$3.535784 \cdot 10^{-2}$	$1.710431 \cdot 10^{-5}$	$4.100642 \cdot 10^{-2}$
	$x_{Proj}[mm]$	$y_{Proj}[mm]$	$z_{Proj}[mm]$	$\theta[^\circ]$
Mean value	225.214132	-1.746786	261.193118	$-1.928191 \cdot 10^{-2}$
Standard deviation	$8.023921 \cdot 10^{-4}$	$3.881600 \cdot 10^{-7}$	$9.305779 \cdot 10^{-4}$	$1.563789 \cdot 10^{-4}$
	$\psi[^\circ]$	$\phi[^\circ]$		
Mean value	40.767629	0.000000		
Standard deviation	$4.695491 \cdot 10^{-3}$	0.000000		

is assumed, that the lens is a perfect lens without distortion and that there exists no displacement of the optical axis with respect to the DMD:

$$\mathbf{k} = \mathbf{0} \quad \wedge \quad x_0 = 0 \quad \wedge \quad y_0 = 0 \ . \tag{20}$$

The values for the position of the pinhole and the DMD were set with a priori knowledge. For the definition of the calibration functional, a reference pattern p_{ref} on the DMD is calculated with the fix edge length of the squares of the projected pattern. The measured values p_{meas} were determined in the following way. At first, the intersections from the straight lines, starting from the transformed and shifted edge points, and running through the pinhole of the projector, and the plane of the DMD were calculated. In the following the intersection points were transformed into the component coordinate system of the projector CS_{Comp} and the distortion, caused by the lens, was computed. In the last step, the displacement of the image focal point was taken account and the points were converted into discrete pixel p_{meas}. Therewith it is possible to define a calibration functional:

$$\epsilon = \|p_{ref} - p_{meas}\|^2 = f(\mathbf{p}) \quad \wedge \quad \min_{\mathbf{p}}(f) \Rightarrow \mathbf{p} \ , \tag{21}$$

with $\mathbf{p}$ as the parameter vector. The minimum of the function f can be found using nonlinear optimisation algorithms, because of the nonlinear character of f.

In the first step of the multi-step-calibration, $\mathbf{p}$ is equal with $\begin{bmatrix} x_{Pin} & y_{Pin} & z_{Pin} & x_{Proj} & y_{Proj} & z_{Proj} \end{bmatrix}$ and $\mathbf{k}$ and $\begin{bmatrix} x_0 & y_0 \end{bmatrix}$ are constant values. In the second step the distortion parameters $\mathbf{k}$ are the variables and the position of the pinhole and the DMD and the focal image point are constant. In the last step $\begin{bmatrix} x_0 & y_0 \end{bmatrix}$ are the unknown parameters. The three steps were executed until a maximum number of iteration steps is reached or the function value of ϵ decreases a pre-defined barrier. The trend of the parameters with respect to the number of iterations is comparable to the trend, shown in Fig. 4. Therewith, the maximum number of iterations is set to 40.

The calibration procedure has been repeated 20 times. The mean value and the standard deviation of the identified parameters are shown in Tab. 2.

The table points out, that the standard deviation of the parameters k_2, k_3, p_1 and p_2 has the same magnitude as the mean value. This implies, that the parameters should not be regarded in the virtual model. Fig. 8 shows the histogramm of the calibration error in pixel and the error map in pixel. The figure points out, that most of the calibration errors are less than 1.5 pixels. The error is slightly bigger than the error of the camera calibration due to the fact, that the inaccuracy from the identification of the camera parameters propagates during the

Table 3. Measurement values of the optical flat

Number	angle [◦]	planarity μm
1	−52.709	13.69
2	−46.385	9.83

Table 4. Measurement values of the groove artefact

Number	angle [◦]	depth mm
1	0.041	1.994

calibration procedure of the projector. For the reason, that most of the errors are less than 1.5 pixels, it can be said, that the calibration was successful.

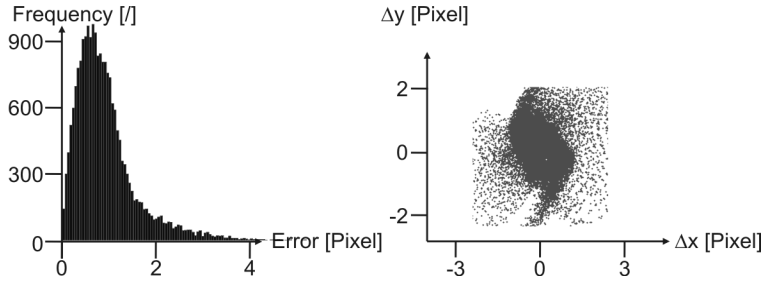

Figure 8. Histogramm and error map from the calibration error after the calibration

4. VERIFICATION OF THE CALIBRATION PROCEDURE

In this chapter, the verification of the calibration procedure will be given. Therefore, an optical flat and a groove artefact will be measured and the planarity and the depth of the groove be determined. In the following the measured values will be compared to the calibrated values.

4.1 Measurement of an optical flat

An optical flat was measured in 2 different positions. The planarity of the flat was calculated using the L_1-norm. The results are given in Tab. 3. The angle is the angle between the normal of the plane and the optical axis of the camera. The table points out, that the planarity is less than $14\mu m$. The optical flat was measured with a coordinate measuring machine (CMM), too. Thereby a planarity of $8.9\mu m$ was determined. Comparing this result with the results, given in Tab. 3, it can be said, that the calibrated fringe projection system yields acceptable results.

4.2 Measurement of a groove artefact

An groove artefact was measured. The depth of the groove was calculated based on a plane-fit of the two planes, using the L_1-norm. The results are given in Tab. 4. The angle is the angle between the normal of the planes and the optical axis of the camera. The depth of the groove was measured with a CMM, too. Thereby a depth of $1.992mm$ was determined. Comparing this result with the result, given in Tab. 4, a deviation between the determined and the calibrated depth of $2\mu m$ exist. Therewith, it can be said, that the calibrated fringe projection system yields acceptable results.

5. CONCLUSION

In this paper, the model of a fringe projection system was described in detail. The model includes all optical parameters, like lens distortions, displacement of the image focal point or the orientation of the optical axes. Subsequent to the description, the calibration procedure and calibration patterns for the identification of all

system parameters was explained. To verify the calibration procedure, the calibration has been repeated 20 times and the standard deviation and the mean values were determined. To verify the whole virtual model, an optical flat and a groove artefact were measured and the planarity and the depth of the groove had been calculated and compared to the calibrated values. The comparison points out, that the measurement deviation between the optical measurement system and a CMM is less than $2\mu m$. This means, that the calibration was successful.

REFERENCES

[1] Hartley, R. I. and Zissermann, A.,[Multiple View Geometry in Computer Vision], Cambridge University Press, (2004)

[2] Schreer, O., [Stereosynthese und Bildanalyse], Springer Verlag, Berlin Heidelberg, (2005)

[3] Valkenburg, R. J. and McIvor, A. M., "Accurate 3D measurement using a structured light system", In: Image and Vision Computing 16, Ausgabe 2, 99 - 110 (1998)

[4] Böttner, T., [Messunsicherheitsbetrachtungen an einem virtuellen Streifenprojektionssystem], Dissertation, Leibniz Universität Hannover, (2009)

[5] Stoer, J., Bulirsch, R., Freund, W. and Hoppe, H. W., [Numerische Mathematik I], Springer Verlag, (2007)

[6] Brown, D.C., "Close-range camera calibration", in Photogrammetrie Engineering, 855 - 866 (1971)

[7] Remondino, F. and Fraser, C.S., "Digital Camera Calibration Methods: Considerations & Comparisons", ISPRS Commission V Symposium Image Engineering and Vision Metrology, (2006)

ACKNOWLEDGMENTS

The authors wish to acknowledge the German Research Foundation (DFG) for the financial support of the subproject B5 of the collaborative reserach centre 489.